ISBN: 978-3-95450-227-1 ISSN: 2673-5490 doi:10.18429/JACoW-IPAC2022-TUOXGD1

DESIGN AND CONSTRUCTION OF OPTICAL SYSTEM OF THE CORONAGRAPH FOR BEAM HALO OBSERVATION IN THE SUPERKEKB

G. Mitsuka*, T. Mitsuhashi, H. Ikeda, KEK, 1-1 Oho, Tsukuba, Ibaraki 305-0801, Japan

Abstract

We developed the coronagraph to measure beam halo in the SuperKEKB electron-positron collider. The coronagraph consists of three stages of optical systems: objective system, re-diffraction system, and relay system. As the coronagraph would be used 60 m downstream of the synchrotron radiation source point, an objective system with a long focal length was required. Because of the dimension of the diamond extraction mirror (20 mm (W) × 23 mm (H)) installed at 23.6 m downstream of the source point, the entrance pupil of the objective system was accordingly limited. To make a coronagraph achieve enough resolution in these constraints, we designed a reflective telephoto system based on the Gregorian telescope for the objective system. The focal length was 7028 mm, and the front principal plane was at the diamond mirror. The re-diffraction and relay systems were also designed based on a Kepler-type telescope. As a result of initial testing using the SuperKEKB electron and positron beams, the performance of the objective system had a diffraction-limited quality, and we achieved a contrast of six orders of magnitude. We present in this paper the early results of the measurements of beam halo at SuperKEKB.

DESIGN AND CONSTRUCTION OF GREGORIAN OBJECTIVE SYSTEM

Obtaining high contrast at the final stage in a coronagraph needs large transverse magnification at the first objective system. As shown in Fig. 1, the location of the coronagraph is 60 m downstream of the synchrotron radiation (SR) source point, and the entrance pupil of the objective system is limited to the aperture of the diamond mirror 20 mm (W) × 23 mm (H). For acquiring high transverse magnification in these conditions, we employ a telephoto system for the objective system. And to eliminate a chromatic aberration, this system adopts a reflective mirror system rather than a refractive lens system.

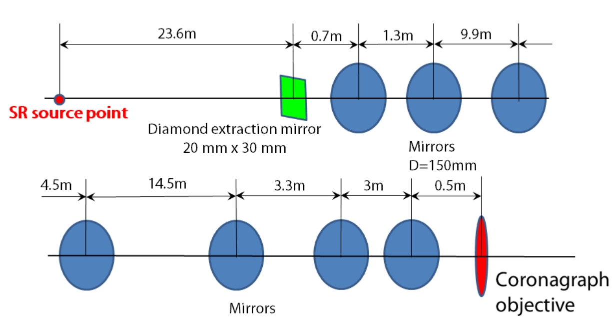

Figure 1: Geometry of the SR visible light optic axis.

* gaku.mitsuka@kek.jp

One choice we consider here is which telescope system we use for the telephoto reflective system: Cassegranian or Gregorian. Our coronagraph chooses a Gregorian system (the top panel of Fig. 2) that uses a parabolic first mirror and an elliptical-concave second mirror (like a shallow parabolic). Making an elliptical-concave mirror is much easier than a hyperbaric-convex mirror employed in a Cassegranian system's secondary mirror.

The bottom panel of Fig. 2 shows the optical design of the objective system. The designed focal length is 7028 mm, the front principal plane is on the diamond mirror, and the distance between the front and rear principal planes is 24 608 mm. The first mirror is a parabolic concave mirror with a focal length of 1200 mm and the second mirror is a shallow elliptical mirror having a focal length of 205 mm.

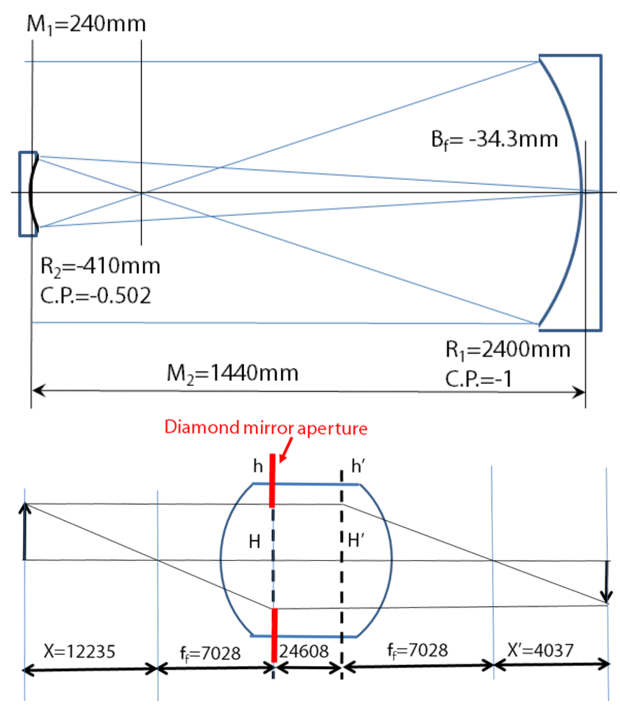

Figure 2: Top: A Gregorian objective system. Bottom: Conjugated system of the objective system.

Another concern in the optics design is scratching and digging on the surfaces of mirrors and lenses, which cause unwanted scattering noises [1]. Less number of lens surfaces in the focusing system reduces scattering noises. Therefore a well-polished singlet lens has been ordinally used in a coronagraph. We applied a special optical polishing to the second elliptical and optical flat mirrors to eliminate scattering sources such as scratch and dig. Note that the first parabolic mirror is made with a normal-grade optical polishing, since primarily the light intensity per area on the mirror

13th Int. Particle Acc. Conf. IPAC2022, Bangkok, Thailand JACoW Publishing
ISBN: 978-3-95450-227-1 ISSN: 2673-5490 doi:10.18429/JACoW-IPAC2022-TUOXGD1

is not as high as the second elliptical mirror, and second, the distance between the mirror surface to the imaging point is long enough.

Before installing it into the coronagraph, we performed a simple knife-edge test to assure the optical performance of the first parabolic mirror and found wavefront error was better than $\lambda/8$ in the entire area of the mirror.

Figure 3 indicates an image of the synchrotron radiation made by the stored beam taken with only the objective system. We see a well-focused beam core in the left panel and more than 15th-order diffraction fringes in the right panel. We conclude that the Gregorian objective system has very diffraction-limited performance.

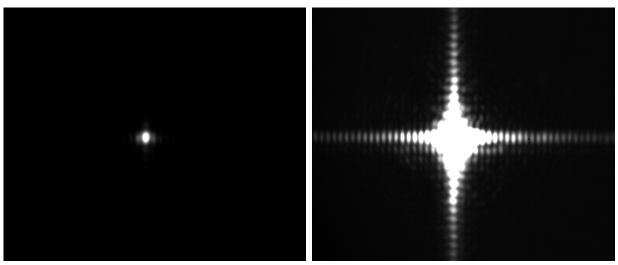

Figure 3: Measurements for synchrotron radiation made with only the objective system. Left: Beam core. Right: Diffraction pattern.

RE-DIFFRACTION SYSTEM

Due to the long distance between the diamond mirror (the entrance aperture of the Gregorian objective system) and the re-diffraction system, large transverse magnification is necessary to obtain enough large image of the entrance aperture at the Lyot stop [2]. As the optical configuration seen in Fig. 4, the optics design follows a Kepler-type telescope for the re-diffraction system.

We use a diffraction-limited doublet with $F = 1000$ mm as an objective lens consisting of 2 groups of 4 lenses with $F = 130$ mm, to magnify the aperture image onto the Lyot stop. The left panel of Fig. 5 shows the aperture images of the re-diffraction system in LER. Since the re-diffraction system is a kind of Schlieren optics, we find typical double-peaked diffraction patterns as a calculation shown in the right panel of Fig. 5.

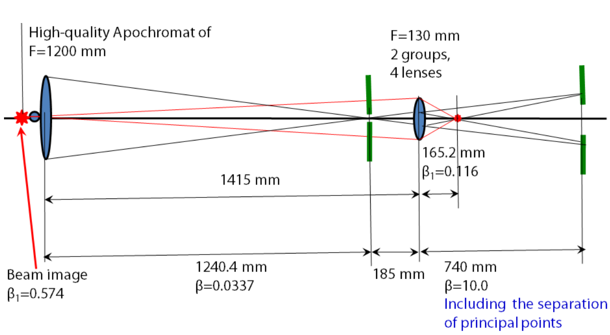

Figure 4: The optical configuration of the re-diffraction system.

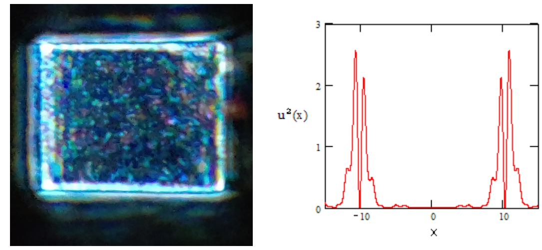

Figure 5: Left: The aperture images of the re-diffraction system. Right: Calculation of diffraction patterns.

RELAY SYSTEM

Downstream at the Lyot stop, a relay system based on a Kepler-type telescope propagates the beam image to a further downstream gated image intensifier camera. As the optical configuration seen in Fig. 6, the system consists of a diffraction-limited doublet having $F = 500$ mm (an objective lens) and magnifier lens $F = 12.5$ mm. Designed value of the transverse magnification of the relay system is 1.

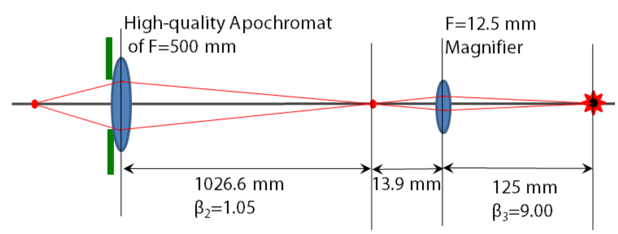

Figure 6: The optical configuration of the relay system.

BEAM HALO MEASUREMENTS

7 GeV Electron Ring (HER)

Before looking at beam halos, we started with test measurements to confirm the coronagraph was correctly in focus and the functions of the opaque square and the Lyot stop. Measurements were performed in 2021 December with the multi-bunch electron single beam at the total beam current 600 mA. The left panel of Fig. 7 shows the gated camera measurement of the HER beam core. The center panel indicates a diffraction pattern generated by the objective system with the $\phi 3$ mm opaque square masking the beam core. As seen in the right panel, the Lyot stop effectively blocks the strong diffraction fringe then the beam halo becomes visible. We took all the three images with the fixed exposure of 10 µs while adjusting the gain of the gated camera.

We made measurements for beam halo for different beam currents as seen in Fig. 8. Since the number of bunchs is always 1370, and the beam current is 75 mA (top left), 200 mA (top right), 390 mA (bottom left), and 790 mA (bottom right), the average bunch current is 0.055 mA, 0.15 mA, 0.28 mA, and 0.55 mA, respectively. We clearly see the beam halo getting visible as the bunch current increases.

ISBN: 978-3-95450-227-1 ISSN: 2673-5490 doi:10.18429/JACoW-IPAC2022-TUOXGD1

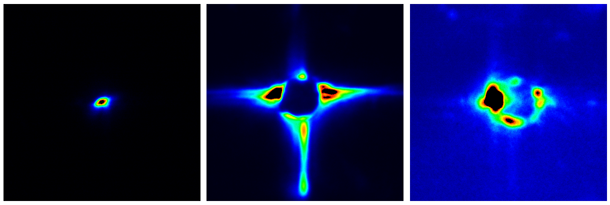

Figure 7: The gated camera measurements for the HER beam. Left: Beam core. Center: Beam core blocked by the ϕ3 mm opaque square, Right: Diffraction fringes are eliminated by the Lyot stop.

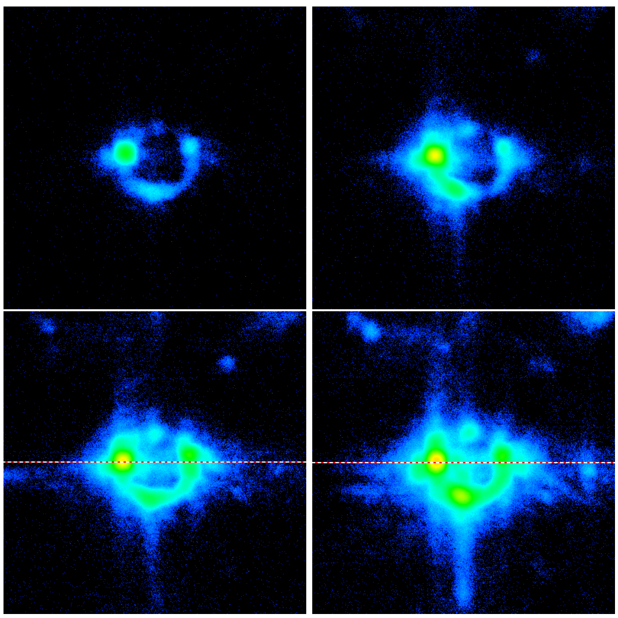

Figure 8: Measurements for beam halos in HER at 75 mA (top left), 200 mA (top right), 390 mA (bottom left), and 790 mA (bottom right).

4 GeV Positron Ring (LER)

Shown in Fig. 9 is a result taken in LER at the beam current 950 mA (average bunch current 0.61 mA). Although patterns of the beam halos in LER irregularly change in each shot, compared with Fig. 8 taken at comparable bunch current in HER, the beam halo in LER is radially available

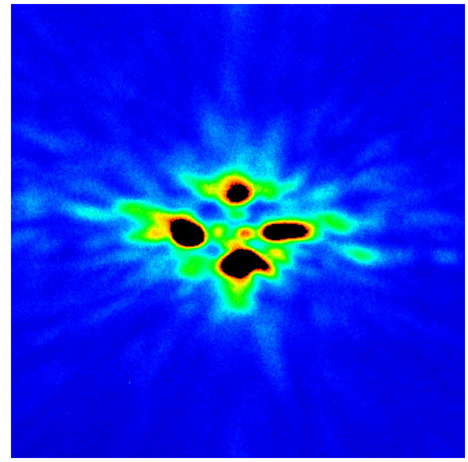

Figure 9: Measurement for beam halos in LER at 950 mA.

away from the beam core and seems stronger than that in HER. This tendency possibly originates in a difference in the beam collision scheme; we made the LER measurements in beam-beam collisions, but no beam-beam collision occurred during the HER measurements. Since the LER energy 4 GeV is lower than the HER energy 7 GeV, beam-beam effects appear more significantly in LER.

In both LER and HER, the maximum intensity in an image taken with blocking the beam core by the opaque square is three orders of magnitude lower than that of the beam core. Extending the exposure time enables measurements for further three orders of magnitude lower radiation. We then achieved the sensitivity of the coronagraph of the six orders of magnitude.

REFERENCES

[1] T. M. Mitsuhashi, "Analysis of Mie Scattering Noise of Objective Lens in Coronagraph for Halo Measurement", in *Proc. IBIC'17*, Grand Rapids, MI, USA, Aug. 2017, pp. 369–372. doi:10.18429/JACoW-IBIC2017-WEPCC10

[2] B. Lyot, "A study of the solar corona and prominences without eclipses", *Monthly Notices of the Royal Astronomical Society*, vol. 99, no. 8, pp. 580–594, 1939. doi:10.1093/mnras/99.8.580